JOURNAL OF CATALYSIS 107, 209–220 (1987)

Alkali-Catalyzed Carbon Gasification Kinetics: Unification of H_2O, D_2O, and CO_2 Reactivities

C. A. MIMS* AND J. K. PABST†

*Exxon Research and Engineering Company, *Corporate Research Science Laboratories, Route 22 East, Annandale, New Jersey 08801, and †Baytown Research and Development Laboratories, P.O. Box 4255, Baytown, Texas 77520*

Received February 10, 1987; revised April 14, 1987

We have been able to quantitatively unify the relative reaction rates for alkali (Li through Cs) salt-catalyzed carbon gasification by H_2O, D_2O, and CO_2. The key to unification is the measurement of catalyst dispersion by a surface alkylation technique in conjunction with the relative rate measurements. After accounting for changes in the catalyst dispersion with gas composition, the reactivity per site is seen to depend only on the oxidizing power of the gas phase. This indicates that the rates are governed by a surface oxidation step in equilibrium with the gas phase which is general to all three reactants. This view is supported by rapid oxygen exchange rates and the form of the rate expressions. The catalyst dispersion decreases with increasing $CO + CO_2$ content of the gas, a fact which we interpret as a change in the morphology of the catalytic salt by CO_3^{2-} formation.

I. INTRODUCTION

The noncatalytic oxidation of solid carbons by H_2O and CO_2 to produce CO is generally thought to proceed in two distinct steps. In the first step a carbon site is oxidized by the reactant gas, and in the second step CO is produced from the oxidized site. Simplest among these schemes is the classic mechanism (1) which has been used extensively to explain the gasification kinetics of carbons (*1–8*):

$$H_2O + \_ \underset{j}{\overset{i}{\rightleftarrows}} H_2 + \underline{O} \qquad [1]$$

$$CO_2 + \_ \underset{j'}{\overset{i'}{\rightleftarrows}} CO + \underline{O} \qquad [2]$$

$$\underline{O} \xrightarrow{k} CO. \qquad [3]$$

Here, _ represents a carbon surface site and $\underline{O}$ represents an oxidized form of the site. The lower case letters are global rate constants. Such a scheme serves to explain much of the kinetic behavior, although the molecular steps involved in these processes are still uncertain.

Such kinetic models have also been applied to the study of gasification catalysis (*8–14*). Because of the additional complexity of catalyzed systems, the nature of the reaction steps is even more difficult to understand. Catalysts have been claimed to affect the reaction pathway in a variety of ways. The action of catalysts has been variously attributed to changes in the identity, number, and reactivity of the surface intermediates. For example, it has been proposed that an iron catalyst mediates the oxidation step by way of bulk phase oxidation–reduction cycles such as Fe ↔ FeO (*2, 9, 15*).

The oxidation–gasification mechanism has been tested in several ways. The individual reaction steps have been examined separately by such techniques as oxygen exchange rate measurements (*3, 11, 16–18*), chemisorption temperature-programmed desorption measurements (*19–23*), and transient experiments (*24–26*). Much work centers around comparison of predicted

0021-9517/87 $3.00

and measured steady-state rate expressions. These include attempts to predict the relative reactivity of several oxidants with the carbon substrate. Such comparisons provide a key check of mechanisms in which two reactants (i.e., H_2O and CO_2) react with the same site.

The predicted relationship between the rates of such reactions is simple when site oxidation (steps 1 and 2) is much faster than step 3, which is generally thought to be the case at moderate pressures. Under these conditions the carbon sites have no memory of whether CO_2, H_2O, or D_2O is the oxidant, and the predicted difference in reactivity of two gases is due solely to their different oxidizing powers. In this limit the model above predicts the following steady-state rate expressions for these two reactions,

$$R = k \cdot \theta \cdot S, \qquad [4]$$

where S is the total number of sites and θ is the steady-state fraction of the sites which are oxidized. θ is governed by the equilibrium constants K_1 and K_2, for reactions 1 and 2, respectively. In the case of H_2O, θ is given by

$$\theta = \frac{[H_2O]}{[H_2O] + [H_2]/K_1} \qquad [5]$$

and in the case of CO_2 is given by

$$\theta = \frac{[CO_2]}{[CO_2] + [CO]/K_2}. \qquad [6]$$

A more general approach when the surface oxidation step is in equilibrium is to cast the problem in terms of the gas phase oxygen atom activity (*27, 28*). The activation of H_2O and CO_2 can be treated as though they first dissociate in the gas phase

$$H_2O \rightleftarrows H_2 + O \qquad [7]$$

$$CO_2 \rightleftarrows CO + O \qquad [8]$$

and the oxygen then reacts reversibly with the surface,

$$O + \_\_ \rightleftarrows \underline{O}. \qquad [9]$$

The oxygen atom activity [O] of ideal H_2O–H_2 and CO_2–CO gas mixtures is then given by

$$[O] = K_7 \frac{[H_2O]}{[H_2]} = K_8 \frac{[CO_2]}{[CO]}. \qquad [10]$$

Both H_2O and CO_2 have similar oxidation potentials at 1000 K with values for K_7 and K_8 of $\sim 10^{-21}$ atm. Surface intermediates involving H_2O and CO_2 are necessary to deliver oxygen atoms to the surface at a measurable rate since gas phase O and O_2 concentrations are too small. The oxygen activity of a gas atmosphere which contains H_2O, H_2, CO, and CO_2 is well defined only if the water gas shift reaction

$$H_2O + CO \rightleftarrows H_2 + CO_2 \qquad [11]$$

is in equilibrium. The relative oxidizing powers of H_2O and CO_2 are thus related to the water gas shift equilibrium constant, $K_{11} = K_7/K_8$.

The functional dependence of the rate on oxygen activity can be quite general. When applied to the limiting case of the mechanism above θ can be written as

$$\theta = \frac{[O]}{[O] + 1/K_9}. \qquad [12]$$

If the rate is linearly proportional to [O] (which is applicable to our results and also corresponds to the low coverage limit in Eq. [12]), then the rate in H_2O–H_2 mixtures reduces to

$$R = k \cdot S \cdot K_7 \cdot K_9 \frac{[H_2O]}{[H_2]} \qquad [13]$$

and in CO_2–CO

$$R = k \cdot S \cdot K_8 \cdot K_9 \frac{[CO_2]}{[CO]} \qquad [14]$$

Inclusion of D_2O as a reactant provides an interesting test of reversible oxidation since D_2O has an oxidizing potential significantly different from that of H_2O. The rate expression for gasification in D_2O–D_2 mixtures can be derived by analogy with Eq.

[7] for dissociation

$$D_2O \rightleftarrows D_2 + O \qquad [15]$$

and with Eq. [13] for the rate

$$R = k \cdot S \cdot K_{15} \cdot K_9 \frac{[D_2O]}{[D_2]}. \qquad [16]$$

In such a model the differences in reactivity of the reactant gases are thus all governed by the appropriate oxidation equilibrium constants. Previous attempts to provide a unified kinetic scheme for these reactions by assuming a common number, identity, and reactivity of the carbon sites have generally failed to provide quantitative agreement with the predictions of such simple models. Ergun and Mentser (*3*), for example, concluded that the number of sites available for the H_2O–carbon reaction was about 60% higher than that for the CO_2–carbon reaction under their conditions although the individual rate expressions were well represented by Eqs. [4]–[6]. However, Grabke (*28*) was able to obtain graphite gasification rates at somewhat higher temperatures in CO_2 and H_2O which agree with the predictions of the simple oxygen activity model above.

In this paper we apply such a treatment generally to the H_2O–carbon and CO_2–carbon reactions catalyzed by alkali metal salts (Li through Cs). The experimental program has two facets. First, selected kinetics data over the range of interest–relative rates of the individual gasification reactions, their gas composition dependence, and oxygen exchange rates—are presented to show consistency with the simple mechanism. Second, postreaction alkylation of samples exposed to selected environments provides a measure of dispersion of the catalyst (*29, 30*) and how it responds to changes in conditions. We find that after accounting for the change in catalyst dispersion with gas composition, the relative rates of gasification in H_2O, CO_2, and D_2O are predicted by simple expressions such as Eqs. [13], [14], and [16].

II. EXPERIMENTAL

Carbon substrates included a high-purity carbon (Spherocarb; Analabs, Inc.), and activated charcoal, as well as char from coal of the Illinois #6 seam. The alkali catalysts were introduced as aqueous solutions of the alkali carbonates. The coal samples were pyrolyzed at 1000 K for 30 min in flowing N_2 after catalyst addition to produce chars. Previous work (*11*) indicated that model carbons and coal chars show similar responses to catalysis by alkali salts.

Rate measurements were performed in a small fixed-bed reactor containing ~250 mg of catalyzed carbon. Water vapor was generated by injecting liquid water from a syringe pump into a heated vaporization zone where it was mixed with metered flows of the other components (H_2, CO_2, CO). We measured gasification rates by gas chromatographic determination of the outlet gas compositions. By using a sufficiently rapid flow rate of the gas mixture we ensured that the reactivity of the gas did not change significantly from the inlet to the outlet of the reactor. For gases containing CO_2 and CO this was somewhat more difficult since the gasifying carbon flux was a small fraction of the flux of carbon through the reactor. For some of the CO_2-containing atmospheres a recirculating pump was used to achieve a well-mixed gas phase in the bed while allowing a more easily measured conversion of the reactant.

When the dependence of the gasification rate on gas composition was examined, the reactant gas was periodically returned to a standard condition in order to monitor any drift in the reactivity of the sample with time. The rates responded in less than 1 min to changes in conditions and showed no appreciable hysteresis when returning to standard conditions. The reactivity of carbon samples catalyzed by the heavier alkalis (K, Rb, Cs) was relatively constant while much of the carbon was gasified. Carbon samples catalyzed by Na and Li

salts, however, generally decreased in rate with carbon conversion. This made time normalization of the data somewhat more difficult since the rate sometimes changed by as much as 40% between successive reference measurements.

We measured the kinetics of oxygen exchange between the gas phase and the surface by isotope exchange techniques. Oxygen exchange in CO_2–CO mixtures was determined by flowing $^{14}CO_2$–^{12}CO mixtures through the bed and measuring the rate of appearance of ^{14}CO in the product by GC-proportional counter. Oxygen exchange in H_2O–D_2 mixtures was determined by measuring the isotopic scrambling with a mass spectrometer. The rates of the forward and reverse water gas shift reactions, also oxygen exchange processes, were also measured. Their rates were measured by GC analysis of the products generated when H_2O–CO and H_2–CO_2 mixtures were flowed through the reactor. Because the rates of oxygen exchange are faster than gasification rates, the measurements were made at generally lower (550 to 950 K) temperatures than those for gasification.

Catalyst dispersion was measured after reaction in selected cases by quenching the sample and reacting with $^{14}CH_3I$ as previously described (*29*). The number of CH_3 groups which reacted with surface salt groups was then determined by combustion of the derivatized samples and measurement of the released $^{14}CO_2$.

III. RESULTS

Oxygen Exchange Kinetics

For the catalytic site to be in oxidation preequilibrium, it is necessary (but not sufficient) that oxygen exchange reactions between the surface and the gas phase be much faster than the gasification rate. These oxygen exchange reactions include water gas shift which must be in equilibrium if a gas containing H_2O, H_2, CO, and CO_2 is to have a well-defined oxygen activity. In addition the oxygen exchange must also involve the gasification site.

We have previously shown that oxygen exchange between CO_2 and CO as well as between H_2O and H_2 on carbons is catalyzed in parallel to gasification by the addition of potassium salts (*11*). These data are reproduced in Fig. 1 for completeness. Addition of incremental amounts of K_2CO_3 to various carbons produces incremental increases in both gasification and the oxygen exchange rates until a saturation amount of catalyst has been added. The catalytic effect is similar for the two carbon substrates. Both reactions show little additional increase in rate as more catalyst is added over the saturation amount. This suggests that the exchange is related to the gasification site. In addition we include data showing that KCl, a relatively ineffective gasification catalyst, is similarly ineffective for oxygen exchange reactions. Orning and Sterling (*17*) measured a catalytic effect of added K_2CO_3 on CO_2–CO exchange over

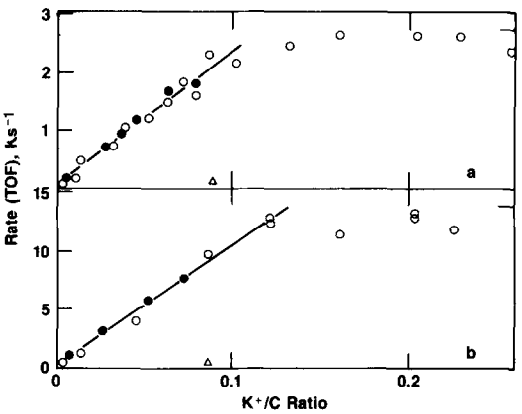

FIG. 1. Response of gasification rate and oxygen exchange rate to potassium catalyst concentration. (a) Gasification rate (carbon atoms gasified per second per carbon atom in the sample) measured in H_2O/H_2 = 1 at 975 K. (b) Exchange rate between CO_2 and CO (turnovers per carbon atom in the sample per second) measured in $^{14}CO_2/^{12}CO$ = 1 at 875 K. The circles are for K_2CO_3 catalyst, open for Illinois coal char, closed for activated charcoal. The triangles are for KCl catalyst. The K/C ratios for Illinois coal char are corrected for the loss of potassium by reactions with coal minerals, principally to form aluminosilicates.

carbons but claimed that physical differences in carbons were as important as catalysis by the alkali. This is obviously not supported by our data.

Figure 2 shows the rates under standard conditions of gasification and oxygen exchange reactions on a potassium-catalyzed Illinois char (K/C = 0.05). The rates, expressed as turnover frequencies per potassium atom, were measured in gas atmospheres consisting of 1 : 1 mixtures of the components indicated and were measured at approximately 20% conversion of the carbon sample. The figure shows that the rates of all the oxygen exchange reactions are two orders of magnitude or more faster than the gasification rates at the same temperature. Notice that at low temperatures the exchange rate in H_2O–D_2 in the absence of CO_2 is much faster than the other oxygen exchange reactions. The addition of 10 mol% CO_2 to the H_2O–D_2 mixture suppresses the exchange rate to values similar to the others. This suggests an interaction at steady state between the catalyst and CO_2 which we discuss in more detail later.

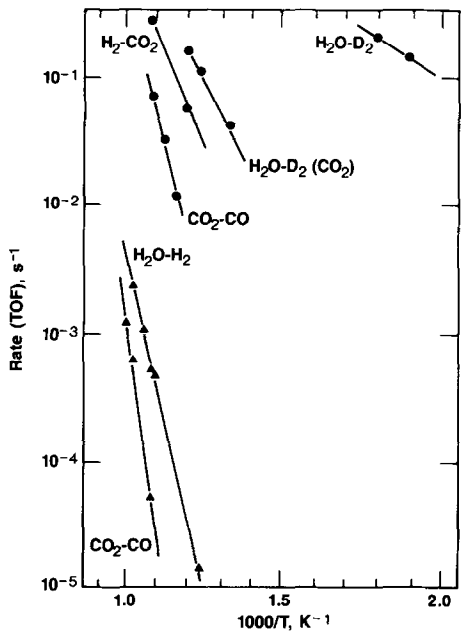

FIG. 2. Turnover frequencies (*per potassium atom*) for gasification reactions (▲) and oxygen exchange reactions (●) in 1 : 1 mixtures of the gases indicated in the figure. The rates were measured on K_2CO_3-catalyzed Illinois coal char (initial K/C = 0.055) after 20–40% of the carbon had been gasified.

TABLE 1

Ratio of Oxygen Exchange Rate to Gasification Rate at 810 K[a]

Alkali	Reactive atmosphere			
	H_2O–D_2	H_2O–D_2(CO_2)[b]	CO_2–H_2	CO_2–CO[c]
Li	1.1×10^{4}[d]	2.2×10^{3}[d]	1.0×10^{3}[d]	—
Na	3.3×10^{5}[d]	4.6×10^{3}[d]	1.2×10^{3}[d]	—
K	3.8×10^{5}	5.3×10^{3}	2.5×10^{3}	3.8×10^{3}
Rb	—	—	4.3×10^{3}	—
Cs	3.6×10^{5}	1.2×10^{4}	4.9×10^{3}	—

[a] Oxygen exchange rates were measured in 1 : 1 mixtures of the gases indicated. Gasification rates were measured in H_2O : H_2 = 1 : 1. Blank entries were not measured.

[b] Oxygen exchange measured in H_2O : D_2 : CO_2 = 1 : 1 : 0.2.

[c] Gasification rate measured in CO_2 : CO = 1 : 1.

[d] Gasification rate extrapolated from 850- to 1000-K temperature range.

Table 1 lists the ratio of oxygen exchange rates to gasification rates at one temperature for carbons catalyzed with the series of alkali carbonates. In all cases the various oxygen exchange rates are much faster than gasification. Because of differences in the rate laws for the gasification and oxygen exchange reactions the ratio of their rates will vary with gas composition (*11, 12*). However, under the conditions of the gasification kinetic studies the oxygen exchange reactions, including water gas shift, were in equilibrium throughout most of the bed (*32*). Therefore, the oxygen activity of the gas was well defined in the gasification rate measurements discussed below.

Gasification Rate Expressions

In this section we present the gas composition dependence of the catalyzed H_2O–carbon and CO_2–carbon reactions. Rate expressions for selected cases have been presented before, sometimes in great detail. The data presented here are intended to show their consistency with the rate expressions in Eqs. [13] and [14].

H_2O–carbon kinetics. Although there have been many studies of the rate expres-

sion of the H_2O–carbon reaction there have been few studies of the rate expression with added catalysts. Most of the kinetics studies have used mechanisms such as Eqs. [1]–[3] to explain the data. Long and Sykes (*10*) generated rather complete kinetic expressions for reaction of H_2O with catalyzed charcoal although the "catalyst" was the suite of adventitious impurities in the material which included alkali. Hydrogen inhibition of the alkali-catalyzed reaction has been noted (*13, 33*). We have previously shown a linear dependence of the potassium-catalyzed reaction on the H_2O/H_2 ratio at 975 K over a limited range of gas composition (*11*).

Figure 3 shows that potassium-catalyzed gasification rates are proportional to the H_2O/H_2 ratio at constant total pressure. Figure 4 shows that there is no dependence of the rate on total pressure at constant H_2O/H_2 ratio. By using sufficiently high flow rates the CO and CO_2 produced by the gasification reaction were kept to levels less than 10 mol% of the hydrogen in the product. At these levels the presence of CO and CO_2 in the gas had no measurable effect on the gasification rate. We verified this by varying the flow rate over a factor of 10 thus producing a tenfold variation in the partial pressures of these product gases. This produced no detectable variation in the gasification rates. As will be discussed later, higher levels of CO and CO_2 (at a given H_2O/H_2 ratio) do have an effect on the rate. Figure 5 shows that a linear dependence on H_2O/H_2 ratio holds for catalytic salts of the other alkali metals. These rates are also normalized to $H_2O/H_2 = 2$.

The rate behavior shown in Figs. 3–5 is thus consistent with the expression given by Eq. [13] as well as that derived from Eqs. [5] and [12] in the regime where oxygen coverage of the sites is low. The rates

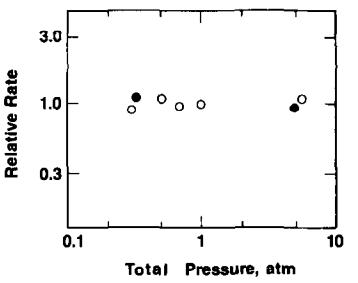

FIG. 4. Dependence of the potassium-catalyzed H_2O–carbon rate on total pressure (at $H_2O/H_2 = 1$). (●) Spherocarb (K/C = 0.03); (○) Illinois coal char (K/C = 0.055).

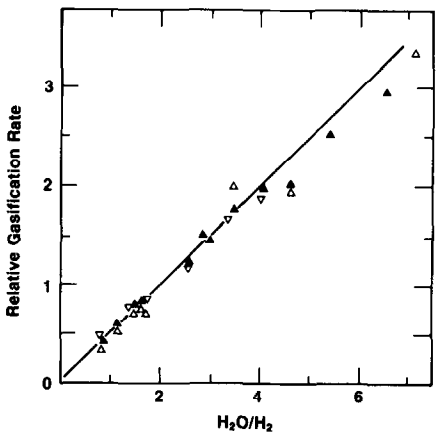

FIG. 3. Dependence of the potassium-catalyzed H_2O–C gasification rate on the H_2O/H_2 ratio under the following conditions: (△) 977 K, 1 atm; (▽) 810 K, 1 atm. Open symbols are for Illinois coal char (K/C = 0.055), solid symbols are for Spherocarb (K/C = 0.03). Rates are normalized to $H_2O/H_2 = 2$.

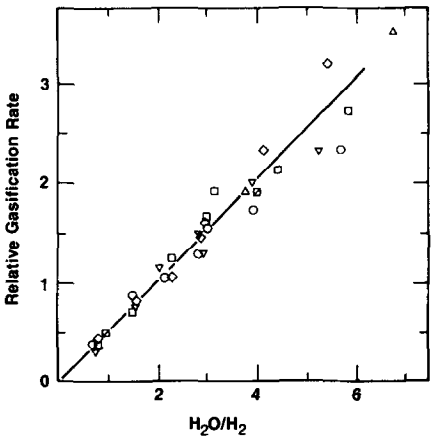

FIG. 5. Dependence of the catalyzed H_2O–C gasification rate on the H_2O/H_2 ratio for different alkali metals. All are measured on Illinois coal char ($M/C \sim 0.05$) at 975 K at 1 atm total pressure. (○) Li^+, (□) Na^+, (△) K^+, (◇) Rb^+, (▽) Cs^+. Rates are normalized to $H_2O/H_2 = 2$.

for all the systems in Figs. 3 and 5 eventually saturate at higher H_2O/H_2 ratios as seen in previous studies and as predicted by the simple mechanism. Some evidence of this can be seen in Fig. 5. These kinetics can be analyzed over an extended range of H_2O/H_2 ratios and pressures to derive other terms in rate expressions predicted by various models. Here, however, we concentrate on demonstrating that the rate behavior in the linear region is due to a reversible oxidation of the surface.

CO_2–carbon kinetics. The few studies of the rate expression of alkali-catalyzed CO_2–carbon reaction are consistent with the foregoing. In addition to the Long and Sykes (*10*) study with a poorly defined catalyst, recent publications show rate expressions with CO inhibition for various catalysts (*8, 12, 13*).

Figure 6 shows that the potassium-catalyzed gasification rate in CO_2 is proportional to the CO_2/CO ratio over a range of oxygen activity similar to that in the H_2O–H_2 case. Again indications of deviation from linear behavior can be seen at high CO_2/CO ratios. Figure 7 shows that the rate

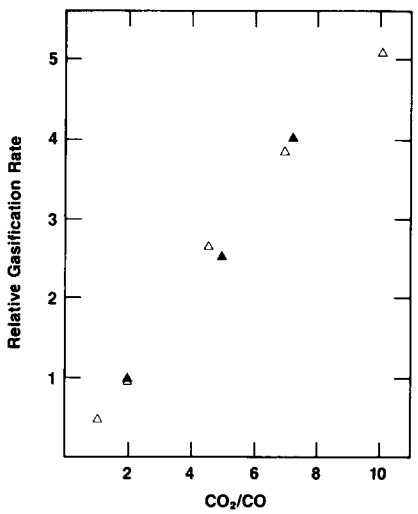

FIG. 6. Dependence of the potassium-catalyzed CO_2–carbon gasification rate on the CO_2/CO ratio. The rates are measured at 977 K, 1 atm on (△) Illinois coal char (K/C = 0.055) and (▲) Spherocarb (K/C = 0.3). The rates are normalized to CO_2/CO = 2.

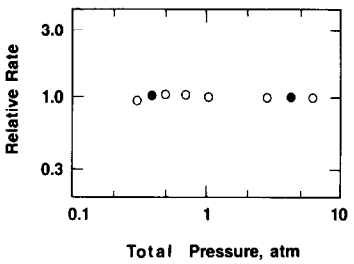

FIG. 7. Dependence of the potassium-catalyzed CO_2–carbon rate on total pressure (at CO_2/CO = 5, 977 K). (●) Spherocarb (K/C = 0.03) and (○) Illinois char (K/C = 0.055).

is independent of total pressure at constant CO_2/CO ratio.

Comparison of Rates in Different Oxidants

The individual rate expressions for the reaction of alkali catalyzed carbons with H_2O and CO_2 are in agreement with the rate expressions generated in the Introduction. The key test of the generality of the simple oxygen activity model is an intercomparison of the reaction rates in different oxidants. The ratios of rates in two different gas compositions were obtained alternating between the two gas compositions (e.g., H_2O–H_2 vs D_2O–D_2) for the life of a carbon sample. The resulting rate ratios were found to be independent of carbon conversion.

H_2O versus D_2O. The ratio of the rate in H_2O–H_2 to that in D_2O–D_2 (for $[H_2O]/[H_2] = [D_2O]/[D_2]$) is predicted by Eqs. [13] and [16] to be equal to K_7/K_{15}. This is simply the equilibrium constant, K_{17}, of the isotope exchange reaction

$$H_2O + D_2 \leftrightarrows D_2O + H_2. \qquad [17]$$

The rate ratios (for $[H_2O]/[H_2] = [D_2O]/[D_2] = 1.0$) for all of the alkali catalysts are shown in Fig. 8 to be in good agreement with the value of K_{17}. Thus we interpret the isotope effect as having a thermodynamic origin rather than a kinetic one. The value of the rate ratio is typical of kinetic isotope effects in H atom transfer reactions (*34*) and

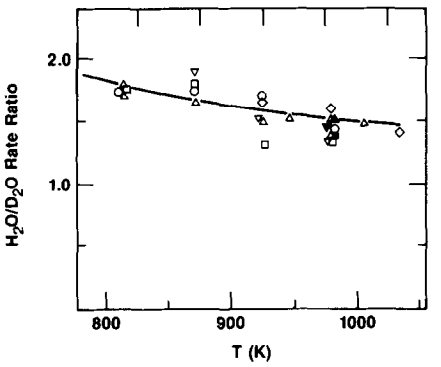

FIG. 8. H_2O/D_2O rate ratios on the catalyzed $H(D)_2O$–carbon reaction for $H_2O/H_2 = D_2O/D_2 = 1$. The ratios are measured at 1 atm total pressure. (○) Li^+, (□) Na^+, (▽) K^+, (◇) Rb^+, (△) Cs^+. Open symbols are for Illinois coal char ($M/C = 0.05$) and closed symbols are for Spherocarb ($M/C = 0.3$). The solid line is K_{17} (see text).

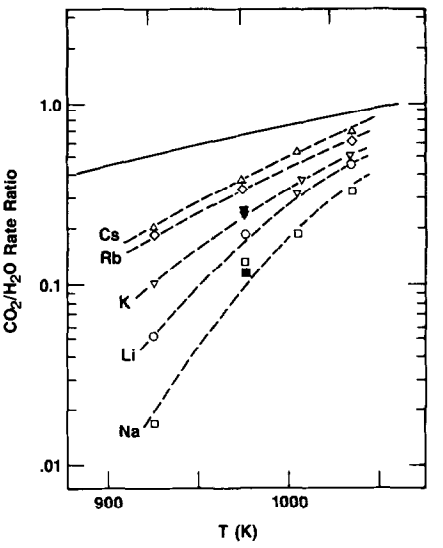

FIG. 9. Ratio of catalyzed gasification rate in CO_2 to that in H_2O for $CO_2/CO = H_2O/H_2 = 1$. The symbols are consistent with those in Fig. 8. The solid line is K_{11}^{-1} (see text).

in a study of the Ba-catalyzed reaction of graphite the $H(D)_2O$ isotope effect was interpreted in this way (*35*). The gas compositions were not reported in this study so that it is not possible to tell whether the data in (*35*) could have been equally well explained as a thermodynamic isotope effect.

H_2O versus CO_2. The ratio of the gasification rate in CO_2–CO mixture to that in H_2O–H_2 (for $[H_2O]/[H_2] = [CO_2]/[CO]$) is predicted from Eqs. [13] and [14] to be K_8/K_7 or $1/K_{11}$, the inverse of the water gas shift equilibrium constant. Figure 9 compares the rate ratios (measured with $[H_2O]/[H_2] = [CO_2]/[CO] = 1$) with $1/K_{11}$ over the temperature range 900–1050 K. The ratios deviate strongly from the prediction at the lower end of the temperature range with more severe disagreement for the lighter alkalis. At higher temperatures all rate ratios tend toward the predicted value.

Figure 9 shows that, compared to gasification rates in H_2O–H_2, the values in CO_2–CO are lower than those predicted by the equilibrium model. Ergun and Mentser (*3*) observed a similar behavior by nominally uncatalyzed carbon and concluded that there were fewer sites to react with the CO_2 than with H_2O. Reactant gas atmospheres which contain substantial fractions of all four species have reactivities intermediate between the simple mixtures. Figure 10 shows this effect for K_2CO_3 and Na_2CO_3-

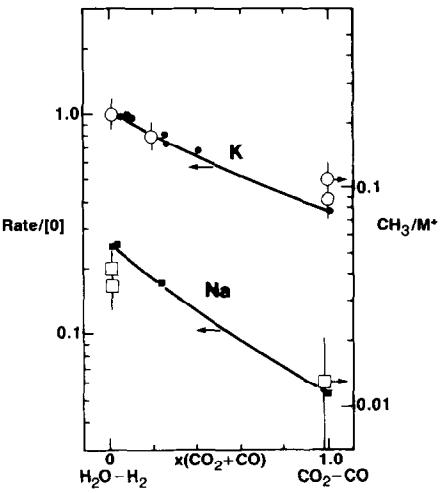

FIG. 10. Comparison of sodium- and potassium-catalyzed gasification rates in various H_2O- and CO_2-containing atmospheres at 975 K with extent of methylation as described in the text. The specific rate data (●, ■) refer to the left ordinate and are connected by the solid lines for visual clarity. They are normalized to H_2O/H_2 K-catalyzed rates. The methylation results (○, □) refer to the right ordinate. All results are for Spherocarb ($M/C = 0.03$).

catalyzed Spherocarb. The relative gasification rates (divided by oxygen activity) are plotted against mole fractions of CO and CO_2 in the gas. The simple oxygen activity model would predict a horizontal line. The effect is a response to mole fraction CO_x (or H_2O/CO_2 ratio) rather than CO_x partial pressure since the specific rates are independent of total pressure (see Figs. 4 and 7).

Figure 9 shows that the CO_2 gasification rate "shortfall" (deviation from that predicted by the simple model) increases as temperature is decreased. We did not extend gasification rate measurements to temperatures below 825 K. However, the degree to which CO_2 suppresses the H_2O–D_2 exchange rate at 675–800 K (Fig. 2) is in rough agreement with the CO_2 gasification rate "shortfall" predicted by extrapolation of the data in Fig. 9. Thus CO_2 in the reactant gas affects gasification and oxygen exchange to a similar degree. The discrepancy between the predictions of the simple model and the relative gasification rates in CO_2 and H_2O can be reconciled if the presence of CO_2 in the reactant gas induces changes in the dispersion of the catalyst. This would also explain the parallel effect of CO_2 on gasification and oxygen exchange rates.

Variation of Catalyst Dispersion with Gas Composition

Alkali-catalyzed carbons which have been quenched from reaction conditions contain large numbers of surface salt groups which will alkylate by reaction with CH_3I (*29*). The formation of these surface groups is associated with the dispersion of the alkali catalyst and explains the reproducible behavior of potassium catalyst on a variety of carbons and with a variety of impregnation techniques (*11*). The number of surface salts correlates with the gasification rate as a function of catalyst concentration (*29, 30*) indicating that this methylation reaction is a good measure of catalyst dispersion. For the moment we set aside questions of whether the surface salts are the active sites for gasification and use the alkylation results simply as a measure of catalyst–carbon contact and therefore proportional to the number of sites, S. The catalyst dispersion measured this way does not depend on the H_2O/H_2 ratio (*30*), in agreement with the simple model (Eq. [13]) and the data in Figs. 3–5.

The effect on the catalyst dispersion of CO–CO_2 mole fraction in the gas was examined by alkylating a series of potassium- and sodium-catalyzed samples after reacting in selected gas compositions represented in Fig. 10. For these experiments, the carbon sample was reacted to 10–20% carbon conversion in the chosen gas mixture. The relative rates just prior to alkylation were consistent with the relative rates obtained by alternation of gas compositions.

These alkylation results are plotted in Fig. 10 along with the rate data. The alkylation results refer to the right ordinate which has been scaled to produce the best overlap with the rate data. The decrease in specific rate with CO–CO_2 content is entirely explained by the decrease in catalyst dispersion. The number of methyl groups on the sodium-catalyzed sample reacted in CO_2 was near the amounts measured for uncatalyzed blank (due in part to residual CH_3I adsorption)—hence the large uncertainty. Quantitative intercomparisons of the various catalysts are outside the scope of this paper. However, the data also illustrate that the difference between absolute rates of the sodium- and potassium-catalyzed samples is due in large part to differences in dispersion as we have previously indicated (*36*). A similar conclusion regarding differences between Na and K catalysts has also been reached recently by different techniques (*24, 37, 38, 42*).

Accompanying the decrease in dispersion of potassium catalyst in CO_2 is an increase in the weight of the catalyst phase. Figure 11 shows the weight change of an uncatalyzed and a K_2CO_3–catalyzed car-

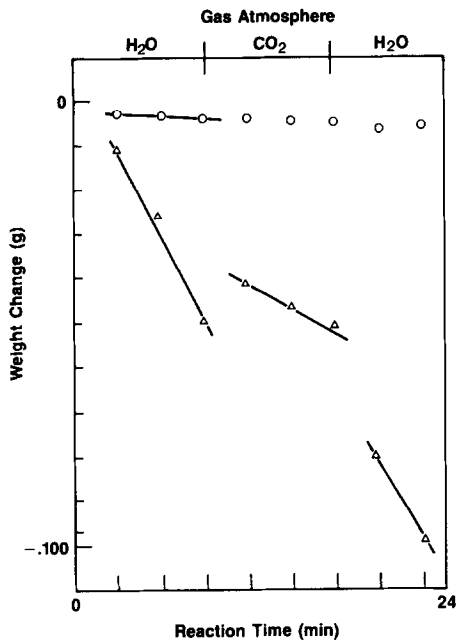

FIG. 11. Weight loss record of uncatalyzed (○) and catalyzed (△) Illinois char (initial K/C = 0.058) after sequential 3-min gasification periods in H_2O and CO_2 at 975 K. The gas atmospheres for the series are indicated at the top of the figure. Initial sample weight in each case = 0.3 g.

bon sample after each of a series of short periods (3 min) of gasification at 975 K. The reaction sequence consisted of a series of exposures in H_2O followed by another series in CO_2 followed by another series in H_2O. After each gasification period, the sample was purged with argon gas and cooled to room temperature in the same manner as that for the alkylation experiments. The entire reactor tube (quartz in these experiments) was removed from the system under argon purge and weighed. The reactor was then reincorporated in the system and the cycle was repeated. Figure 11 shows that the catalyzed sample actually gained weight in the first gasification period after changing from H_2O to CO_2. Extrapolation of the rate of weight loss in CO_2 back to the time of the switch in gas composition indicates an incremental weight increase of ~15 mg which is apparently lost upon reintroduction of H_2O. A similar weight change is not seen when the same series of experiments is repeated on an uncatalyzed sample. The incremental weight must therefore be associated with the catalyst. If the incremental weight is assumed to be CO_2, the 15 mg corresponds to approximately 0.3 CO_2 per potassium atom.

IV. DISCUSSION

Over the range of conditions studied here, knowledge of the catalyst–carbon contact and the oxygen activity of the gas has allowed us to unify the kinetics of alkali salt-catalyzed gasification rates in H_2O, D_2O, and CO_2. The rate can be written as a separable function $R = k' \cdot S \cdot [O]$. The number of sites, S, is influenced by gas composition, while the turnover frequency per site depends on the oxygen atom activity.

The changes in catalyst dispersion documented in Fig. 10 are rapid, reversible accommodations of the catalyst to changes in gas composition. We have not considered the more or less irreversible variation of the catalyst dispersion with other parameters such as carbon conversion and impregnation technique. The catalyst dispersion depends on these parameters in a complex manner depending on the identity of the alkali metal and conditions (*23, 39, 40*).

With K, Rb, and Cs carbonates a rather reproducible catalyst dispersion is achieved. A significant fraction of the catalyst is associated with surface salts of functional groups on the carbon substrate. For active potassium in H_2O–H_2 atmospheres typically one surface salt exists on the carbon substrate for every four to five potassium atoms at 1000 K. The remainder of the alkali exists in a noncrystalline state with associated oxygen (*19, 30, 38*). There have been several conjectures in the literature as to the form of this inorganic phase. These include salt clusters solvating the surface salt and molten salt films, possibly of oxygen-deficient alkali oxides as proposed by Wood *et al.* (*41*). The catalyst

phase is quite mobile under reaction conditions and can rapidly accommodate to changes in the gas phase composition. The introduction of a reactant atmosphere containing large amounts of CO + CO_2 to the gas phase at 975 K reduces the number of surface salts to approximately one for every 10 potassium atoms. This reversible change in catalyst dispersion in CO_2 is likely caused by a change in the suite of inorganic anions associated with the catalyst, possibly by production of CO_3^{2-} from O^{2-} and OH^-. The presence of CO_3^{2-} anions in the catalyst phase would be expected to affect the average cluster size or the film thickness at steady state. Lang (*42*) has invoked competition between carbonate and a hydrolyzed form of the catalysts to explain anion effects in catalyzed gasification. This is supported by the weight gain shown in Fig. 11. If one supposes that the weight gain reflects removal of active potassium $2K^+ (+ O^{2-}) + CO_2 \Rightarrow K_2CO_3$, the measured stoichiometry 0.3 CO_2 per potassium atom corresponds to a reduction in activity by 60%, similar to the measured decrease in dispersion. Formation of bulk K_2CO_3 is not seen by X-ray diffraction, however. Furthermore, *in situ* X-ray adsorption edge (NEXAFS) measurements of Rb catalyst in CO_2 at 950 K show the Rb environment to be distinct from bulk Rb_2CO_3 (*43*). At this temperature rubidium shows "inhibition" by CO_2/CO comparable to potassium (see Fig. 9). Therefore the absence of carbonate signature in the NEXAFS is puzzling.

The kinetics presented here show that the oxidation of the gasification site is equilibrated under the conditions of this study. The actual chemistry of the surface oxidation is uncertain. It could be site specific as implied in simple mechanisms like Eqs. [1]–[3] or it could be nonlocal and similar to the electrochemical mechanism proposed by Rao *et al.* (*18*). We favor a mechanism wherein the surface phenoxides associated with the catalyst are in fact gasification intermediates. In this model the phenoxides are reversibly oxidized to phenoxy radical analogs (Scheme 1) with the phenoxy analog decomposing to give CO (Scheme 2).

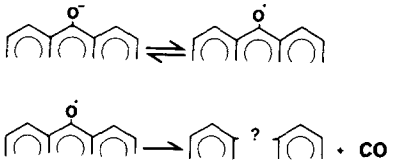

This mechanism is electrochemical in character with the catalyst phase acting as an electrolyte. The stabilization of surface phenoxide analogs by the basic salt phase provides a suitable precursor for CO evolution. In addition, the fact that the oxidized site (phenoxy) is in equilibrium with the gas phase oxidation potential provides a rationalization for the similarity in rate parameters among the different alkali metals shown in Fig. 10 and reported elsewhere (*8, 12*).

ACKNOWLEDGMENTS

We thank W. Robbins for the ^{14}C determinations. We also thank Jack Crawford and Barbara Hinojosa for technical assistance.

REFERENCES

1. Gadsby, J., Hinshelwood, C. N., and Sykes, D. K., *Proc. R. Soc. London Ser. A* **187,** 129 (1946); Gadsby, J., Long, F. J., Sleightholm, P., and Sykes, K. W., *Proc. R. Soc. London Ser. A* **193,** 357 (1948).
2. For reviews see (a) Walker, P. L., Jr., Rusinko, F., Jr., and Austin, L. G., "Adv. Catalysis" (O. D. Eley, P. W. Selwood, and P. B. Weisz, Eds.), Vol. 11, pp. 133–221. Academic Press, New York, 1959; (b) von Fredersdorff, C. G., and Elliot, M. A., *in* "Chemistry of Coal Utilization" (H. H. Lowry, Ed.), Suppl. Vol., Chap. 20, p. 892. Wiley, New York, 1963; (c) Laurendeau, N. M., *Prog. Energy Combust. Sci.* **4,** 221 (1978).
3. Ergun, S., and Mentser, M., *Chem. Phys. Carbon* **1,** 203 (1965).
4. Mentser, M., and Ergun, S., *Carbon* **5,** 331 (1967).
5. Strange, J. F., and Walker, P. L., Jr., *Carbon* **14,** 345 (1976).
6. Yang, R. T., and Yang, K. L., *Carbon* **23,** 537 (1985).
7. (a) Koenig, P. C., Squires, R. G., and Laurendeau, N. M., *Carbon* **23,** 531 (1985); (b) *Fuel* **65,** 412 (1986).
8. Freund, H., *Fuel* **64,** 657 (1985).

9. For reviews of catalytic gasification mechanisms see McKee, D. W., *Chem. Phys. Carbon* **16,** 1 (1981); for a specific review of alkali catalysts see Wood, B., and Sancier, K. M., *Catal. Rev. Sci. Eng.* **26,** 233 (1984). Also see the special issues of *Fuel* which contain the proceedings of the International Symposia "Fundamentals of Catalytic Coal and Carbon Gasification," Volume 63, No. 2 (February, 1983) and Volume 65, No. 10 (October, 1986).
10. Long, F. J., and Sykes, K. W., *J. Chim. Phys.* **47,** 361 (1950).
11. Mims, C. A., and Pabst, J. K., *Amer. Chem. Soc. Div. Fuel Chem. Prepr. Pap.* **25**(3), 258, 263 (1980).
12. (a) Kapteijn, F., Peer, O., and Moulijn, J. A., *Fuel* **65,** 1371 (1986); (b) Cerfontain, M. B., and Kapteijn, F., *Fuel* **63,** 1043 (1984); (c) Kapteijn, F., and Moulijn, J. A., *Fuel* **62,** 221 (1983).
13. Schumacher, W., Muhlen, M. J., van Heek, K. H., and Jüntgen, H., *Fuel* **65,** 1360 (1986).
14. Koenig, P. C., Squires, R. G., and Laurendeau, N. M., *J. Catal.* **100,** 228 (1986).
15. Herman, G., and Hüttinger, K. J., *Fuel* **65,** 1410 (1986).
16. Bonner, F., and Turkevich, J., *J. Amer. Chem. Soc.* **73,** 561 (1951).
17. Orning, A. A., and Sterling, E., *J. Phys. Chem.* **58,** 1044 (1954).
18. Rao, M. B., Vastola, F. J., Walker, P. L., Jr., *Carbon* **21,** 401 (1983).
19. Saber, J. M., Falconer, J. L., and Brown, L. F., *J. Catal.* **90,** 65 (1984); *Fuel* **65,** 1356 (1986).
20. Delannay, F., Tysoe, W. T., Heinemann, H., and Somorjai, G. A., *Carbon* **22,** 401 (1984).
21. Kapteijn, F., Abbel, G., and Moulijn, J. A., *Fuel* **63,** 1036 (1984).
22. Kelemen, S. R., and Freund, H., *Amer. Chem. Soc. Div. Fuel Chem. Prepr. Pap.* **30,** 286 (1985).
23. Ratcliffe, C. T., and Vaughn, S. N., *Amer. Chem. Soc. Div. Fuel Chem. Prepr. Pap.* **30,** 304 (1985).
24. Cerfontain, M. B., Meijer, R., and Moulijn, J. A., "Proc. Int. Conf. Coal Sci. Sydney, 1985," p. 277. Pergamon, New York, 1985.
25. Freund, H., *Fuel* **65,** 63 (1986).
26. Sy, O., and Calo, J. M., *Amer. Chem. Soc. Div. Fuel Chem. Prepr. Pap.* **28,** 6 (1983).
27. A review of dissociated atom reactivities in gas solid reactions including carbon gasification is contained in Wagner, C., *Adv. Catal.* **21,** 323 (1970).
28. (a) Grabke, H. J., *Ber. Bunseng. Phys. Chem.* **70,** 664 (1966); (b) Grabke, H. J., *Carbon* **10,** 587 (1972).
29. Mims, C. A., Rose, K. D., Melchior, M. T., and Pabst, J. K., *J. Amer. Chem. Soc.* **104,** 6886 (1982).
30. Mims, C. A., and Pabst, J. K., *Fuel* **62,** 176 (1983).
31. Hüttinger, K. J., Masling, R., and Minges, R., *Fuel* **65,** 932 (1986).
32. This was found at longer residence times by Lewis, W. K., Gilliland, E. R., and Hipkin, H., *Ind. Eng. Chem.* **45,** 1697 (1953).
33. Hüttinger, K. J., and Minges, R., *Fuel* **65,** 1122 (1986).
34. Johnston, H. S., "Gas Phase Reaction Rate Theory," Ronald, New York, 1966; Ozaki, A., "Isotope Studies of Heterogeneous Catalysis," Kondasha Ltd., Tokyo, and Academic Press, New York, 1977.
35. Yates, J. T., Jr., and McKee, D. W., *J. Chem. Phys.* **75,** 2711 (1981).
36. Mims, C. A., and Pabst, J. K., "Proc. Int. Conf. Coal Sci., Düsseldorf, 1981," p. 730. (verlag Glückauf GmbH, Essen, 1981)
37. Hashimoto, K., Miura, K., Xu, J. J., Watanabe, A., and Masukami, H., *Fuel* **65,** 489 (1986).
38. Yokoyama, S., Miyara, K., Tanaka, K., Tashiro, J., and Takakuwa, I., *Nippon Kagaku-Kaishi* 974 (1980).
39. Radovic, L., and Walker, P. L., Jr., *Fuel* (1984).
40. Bruno, G., Carvani, L., and Passoni, G., *Fuel* **65,** 1368 (1986).
41. Wood, B. J., Fleming, R. H., and Wise, H., "Proc. Int. Conf. Coal Science, Pittsburg, 1983," p. 415.
42. Lang, R. J., *Fuel* **65,** 1324 (1986).
43. Mims, C. A., and Cramer, S. P., paper 30f, AIChE Annual Meeting, San Francisco, November, 1985.
44. Jalan, B. P., and Rao, Y. K., *Carbon* **16,** 175 (1978).